Frontiers in Bioscience Landmark

Front. Biosci. (Landmark Ed) **2022**; 27(11): 305
https://doi.org/10.31083/j.fbl2711305

Original Research

Preliminary Analysis of the Presence of Bacterial Azurin Coding Gene in CRC Patients and Correlation with the Microbiota Composition

Marta Iozzo[1], Francesco Vitali[2], Carolina Chiellini[3], Leandro Gammuto[4], Antonio Taddei[5], Amedeo Amedei[5,*], Renato Fani[6,*]

[1]Department of Experimental and Clinical Biomedical Sciences, University of Florence, 50134 Florence, Italy
[2]Research Centre for Agriculture and Environment, Council for Agricultural Research and Economics, 50125 Firenze, Italy
[3]Institute of Agricultural Biology and Biotechnology, National Research Council, 56124 Pisa, Italy
[4]Department of Biology, University of Pisa, 56126 Pisa, Italy
[5]Department of Experimental and Clinical Medicine, University of Florence, 50134 Florence, Italy
[6]Laboratory of Microbial and Molecular Evolution, Department of Biology, University of Florence, 50019 Sesto Fiorentino (Firenze), Italy
*Correspondence: amedeo.amedei@unifi.it (Amedeo Amedei); renato.fani@unifi.it (Renato Fani)
Academic Editor: Ru Chen
Submitted: 7 July 2022 Revised: 1 October 2022 Accepted: 1 November 2022 Published: 11 November 2022

Abstract

Background: Azurin, a bacterial cupredoxin firstly isolated from the bacterium *Pseudomonas aeruginosa*, is considered a potential alternative therapeutic tool against different types of cancer. **Aims**: In this work we have explored the relationship possibly existing between azurin and colorectal cancer (CRC), in light of the evidence that microbial imbalance can lead to CRC progression. **Methodology/Results**: To this aim, the presence of azurin coding gene in the DNA extracted from saliva, stool, and biopsy samples of 10 CRC patients and 10 healthy controls was evaluated by real-time PCR using primers specifically designed to target the azurin coding gene from different bacterial groups. The correlation of the previously obtained microbiota data with real-time PCR results evidenced a "preferential" enrichment of seven bacterial groups in some samples than in others, even though no statistical significance was detected between controls and CRC. The subset of azurin gene-harbouring bacterial groups was representative of the entire community. **Conclusions**: Despite the lack of statistical significance between healthy and diseased patients, HTS data analysis highlighted a kind of "preferential" enrichment of seven bacterial groups harbouring the azurin gene in some samples than in others.

Keywords: azurin; *Pseudomonas aeruginosa*; colorectal cancer; real-time PCR; microbiota

1. Introduction

At the end of the 19th century bacteria and their metabolites were tested for the first time as anticancer agents [1,2]. This interest in the development of alternative therapies based on the use of bacteria and/or their secondary metabolites has renewed and increased in the last years. Indeed, some bacterial (secondary) metabolites have been found to specifically affect the tumor cells survival or, otherwise, interfere with signalling pathways that allow cancer progression [3–7].

Among these, cupredoxins are metalloproteins involved in bacterial electron transport chain [8,9] showing different activities including antimalarial [10] and anticancer ones [5,11–15]. The cupredoxin family includes azurins, rusticyanins, pseudoazurins, auracyanins, amicyanins, and halocyanins [16,17]. For several decades, the interest in anticancer activity has mainly focused on azurin [5,14,18]. Even though Azurin was purified in 1958 [19], it was discovered for the first time in *Pseudomonas aeruginosa*, where it is secreted as periplasmatic protein [5]. Azurin belongs to the copper proteins type 1, and it is involved in the electron transfer chain within the denitrification process in *P. aeruginosa* [3,20,21]. This protein has a tertiary β-barrel structure, and, in a pathological context, preferentially enters in human cancer cells rather than the healthy ones [7,21–23]. This selective internalization seems to be dependent on the enrichment of cholesterol microdomains (lipid raft) that are commonly over-expressed in tumor cells [5] since its depletion significantly reduced its cellular penetration [5,24]. The preferential azurin entry in tumor cells is mediated by the peptide p28 (Leu50-Asp77) representing the azurin's transport protein domain. P28 is composed of an extended amphipathic helix [25]. It has been shown that p28 entry in cancer cells mainly occurs *via* endocytic pathway and without loss of membrane integrity [24,26,27]. Besides p28, there are other less studied azurin-derived peptides, known as p12 (Gly66-Asp77), p18b (Val60-Asp77) and p18 (Leu50-Asp77); both p12 and p18b lack of cell penetration ability, while p18 has got the ability to preferential penetrate into the cancer cells [24,28,29]. In this scenario, the most studied azurin-associated peptide is p28. Once azurin or p28 enter cancer cells, they induce multiple anticancer effects such as apoptosis, anti-proliferative potential, arrest of cell cycle, as well as impair angiogenesis [7,26,30,31].

Besides, different *in vivo* studies demonstrated that azurin and p28 inhibit tumor growth in 4T1 breast model, B16 melanoma and Dalton's lymphoma ascites model [30,32,33].

More in-depth, regarding *in vitro* evidence, azurin/p28 can induce inhibition of cancer cells proliferation *via* p53 pathway, by complexing and stabilizing p53, inducing overexpression of pro-apoptotic genes such as *BAX*, and, consequently, decreasing BCL-2 level that leads to the release of mitochondrial cytochrome c in the cytosol, thus promoting downstream activation of apoptotic machinery [30,34–37]. Despite this activity has been demonstrated *in vitro*, mainly in breast, colon, melanoma, glioblastoma, and prostate cancer cell lines [24,30,31,35,38–41] the proliferation inhibition was observed also in other cancer cell lines such as ovarian cancer, fibrosarcoma, osteosarcoma, pancreatic cancer, and neuroblastoma [24,31,42].

In addition, azurin improves anticancer response also through modulation of cell membrane properties, impacting for instance on β1 integrin expression level in lung cancer models and, consequently, enhancing the responsiveness to EGFR-target therapy [43]. More recently, Bernardes and co-workers [40] discovered an interaction between azurin and lipid raft components (ganglioside GM-1, caveolin-1): accordingly, azurin-treatment decreases caveolin-1 expression and plasma membrane order, subsequently enhancing the response to chemotherapeutic drugs activity (paclitaxel, doxorubicin) in both MCF-7 and HeLa cells [40]. In a P-cadherin overexpressing breast cancer model, the same group demonstrated that azurin decreases invasion ability and impairs FAK/Src signalling [38,39].

Considering these promising evidence, two recent clinical trials (phase I) have been completed [44,45], demonstrating the efficacy of a safety and optimal dose of p28 on (i) 15 patients bearing metastatic solid tumors - NCT00914914; (ii) 18 younger patients with recurrent or progressive central nervous system tumors - NCT01975116.

Recent studies have highlighted how azurin is able to impact on cellular processes such as adhesion and invasion of bacterial pathogens (e.g., *S. aureus*, *Salmonella* sp.) in Colorectal Cancer (CRC) lines CaCo-2 [20]. The azurin involvement in bacterial-cancer cell interactions was demonstrated for CRC through experiments of exclusion, competition, and replacement. These results paved the way to innovative ideas for potential adjuvant therapies. Moreover, regarding CRC pathogenesis, an involvement of the gut microbiota in CRC development and therapy response is documented [46]. Accordingly, increasing evidences from metagenomic analyses highlighted a microbial imbalance (dysbiosis) typical of the CRC patient gut, that supports a pathological state [47]. Recently, the analysis of exopolysaccharides (EPSs) activity from *Pseudomonas* sp. strains against HT-29 CRC cell line, confirmed that microbial molecules are able to carry out anti-tumor activity in CRC through apoptosis mechanism [48].

Surprisingly, there is a considerable lack of investigation about azurin gene and protein in biological samples of human origin, especially related to the occurrence of cancer. An enrichment in azurin gene content of the microbiota in the cancer context, could suggest that the azurin is able to confer a selective advantage to such microorganisms. This evidence, in turn, could be leveraged to induce enrichment in azurin-harbouring microorganisms, potentially leading to an in-situ production of azurin able to have a pharmacological value for the host.

In this work, samples collected from CRC patients and healthy controls [49] were analysed for the presence of specific bacterial groups related to the production of azurin. The analysis was conducted on High-throughput sequencing (HTS) data previous collected for the FAS project "MICpROBIMM" [49], and *via* quantitative amplification protocol by real-time PCR. Six primer pairs specifically designed to target the azurin gene from different bacterial groups (mainly different *Pseudomonas* species) were designed and validated through end-point PCR. Four of the validated primer pairs were used for quantitative real-time PCR in samples collected from 10 colorectal cancer patients (saliva, stool and biopsy samples), in comparison with samples collected from 10 healthy subjects (in saliva and stool samples). Our aim was therefore to evaluate the presence of azurin gene in the available samples, to evaluate any differences in relation to the sample type and also in relation to the bacterial groups producing azurin.

2. Materials and Methods

2.1 Primer Design and Validation

The primer sets for azurin amplification were designed based on the conserved regions obtained from the alignment of the azurin nucleotide sequences using the BioEdit software version 7.2.6 [50]. For the primer design the following parameters were considered: 18–25 base pairs length, a similar denaturation temperature of the primer forward with the primer reverse in each couple (Tm) and the nucleotide composition of the primer sequences, whose GC content was established as being about 60% [51]. A total of 6 primer pairs were designed (Table 1).

2.2 End-Point PCR Condition for Primer Pairs Validation

The 6 primer pairs were validated through end-point PCR on a panel of bacterial strains that were present in the laboratory collections of the Dept. of Biology, University of Florence. The strains used are listed in Table 2 (Ref. [52–54]). The amplification with the designed primer pairs were performed in 20-μL reactions using DreamTaq DNA Polymerase reagents (Thermofisher Scientific, Waltham, MA, USA) at the concentrations suggested by the company, and 0.5 μM of each primer. 1 μL of bacterial cells lysate was used as a template for each reaction. The amplification conditions were the following: 5 minutes denaturation at 95 °C,

Table 1. Characteristics of the six primer pairs designed in this study for the specific amplification of a portion of the azurin protein-coding gene.

	PRIMER PAIRS					
	Pseudomonas aeruginosa	*Pseudomonas* group 12	*Pseudomonas* group 1	P*seudomonas* group 4	*Aeromonas*	*Pseudomonas* group 5
Primer forward (F)	5′-GGCTGCCGAGTGCTCGG-3′	5′-AAGAGCTGCAAGACCTT-3′	5′-ATGAYTCGCAAGCTTGTA-3′	5′-ATCGACAAGAGCTGCAAG-3′	5′-CATGGGYCACAACTGGG-3′	5′-ATGTTTGCCAAACTCGT-3′
Primer reverse (R)	5′-CCCTGCATGTCGGCGGC-3′	5′-GGGAAGGAGCAGAAGA-3′	5′-GCGCCTTTCATCATGCT-3′	5′-CCTTTCATCATCGAGATRT-3′	5′-CCGGGGAAGGAGCAGAA-3′	5′-GTTRTGVCCCATSACGTT-3′
Tm primer F	62 °C	50 °C	50 °C	54 °C	56 °C	48 °C
Tm primer R	62 °C	50 °C	52 °C	52 °C	57 °C	50 °C
Annealing temperature in PCR	62 °C	50 °C	50 °C	52 °C	56 °C	48 °C
Target	*P. aeruginosa*	*P. fluorescens, P. cichorii, P. coronafaciens, P. delhiensis, P. pseudoalcaligenes, P. mendocina*	*P. syringae, P. savastanoi, P. amygdali, P. cannabina*	*P. fluorescens, P. marginalis, P. putida, P. simiae, P. trivalis, P. costantinii*	*A. aquatica, A. caviae, A. fluvialis, A. hydrophila, A. rivuli, A. salmonicida.*	*P. fluorescens, P. sp., P. cedrina, P. chlororaphis, P. protegens*
N. of target sequences	2290	98	268	221	195	143
Fragment length (bp)	177	275	431	305	216	201

Table 2. List of the bacterial strain used for primer pairs validation in end-point PCR.

Strain	Source	Taxonomy	Reference
3.33	Acquarossa river, red epilithon	*Pseudomonas* sp.	[52]
5.14	Acquarossa river, black epilithon	*Pseudomonas chloraphis*	[52]
11.7	Infernaccio waterfalls, red epilithon	*Pseudomonas fluorescens/P. protegens*	[52]
2.13	Acquarossa river, red epilithon	*Pseudomonas fluorescens/P. protegens*	[52]
14.6	Infernaccio waterfalls, red epilithon	*Pseudomonas moraviensis*	[52]
3.18	Acquarossa river, red epilithon	*Aeromonas* sp.	[52]
11.45	Infernaccio waterfalls, red epilithon	*Aeromonas* sp.	[52]
11.47	Infernaccio waterfalls, red epilithon	*Aeromonas* sp.	[52]
Ep_R1	Echinacea purpurea roots	*Pseudomonas* sp.	[53,54]
ATCC 9027	Department of Health Sciences, University of Florence, Laboratory of Prof. A. Lo Nostro.	*Pseudomonas aeruginosa*	
4739	Department of Health Sciences, University of Florence, Laboratory of Prof. A. Lo Nostro.	*Pseudomonas aeruginosa*	
5254	Department of Health Sciences, University of Florence, Laboratory of Prof. A. Lo Nostro.	*Pseudomonas aeruginosa*	

30 cycles of 30 s at 95 °C, 30 s at the annealing temperature specific for each primers pair (Table 1) and 30 s at 72 °C, followed by a final extension of 10 min at 72 °C. In order to check whether the primer pairs correctly amplified the azurin gene, some randomly chosen amplicons were purified and sequenced by using the same primer pairs used in the end-point PCR; the obtained sequences were compared with those available in databases, in order to determine their correspondence with bacterial azurin gene. The obtained sequences are available as supplementary material.

2.3 Set-up of Real-Time PCR Protocol with the Chosen Primer Pairs

Real-time PCR reactions were performed on a panel of samples collected from CRC, and healthy subjects (HC, Table 3, Ref. [49]), in a QuantStudioTM 7 apparatus (Applied Biosystems, Waltham, MA, USA), using a SYBR Green mix (Thermo Fisher Scientific), and according to the protocol described in Checcucci *et al*. [55]. Four out of the six primers pairs were chosen for real-time PCR on samples listed in Table 3, namely: "*Pseudomonas* group 4", "*Pseudomonas* group 5", "*Pseudomonas* group 12" and "*Pseudomonas aeruginosa*". The choice was made on the basis of the end-point PCR results. For each primers pair, a standard curve was constructed starting from the corresponding azurin amplicon, that was previously quantified. Amplicon quantifications were performed with GelQuant.NET software provided by biochemlabsolutions.com (http://biochemlabsolutions.com/GelQuantNET.html). The copy number of azurin amplicon in each point of the standard curve and in samples giving a positive signal was calculated using the free software "dsDNA copy number calculator" (https://cels.uri.edu/gsc/cndna.html).

2.4 Analysis of the Distribution of the Bacterial Groups Producing Azurin in the High Throughput Sequencing Dataset

Raw sequencing data obtained in Russo *et al*. [49] were downloaded from the SRA database using fastq-dump command in the SRA-Toolkit and using the accession numbers (SRR) associated to the single samples included in the BioProject at accession PRJNA356414 (SRA accession SRP094636). According to Vitali *et al*. [56], the obtained sequence fastq files were pre-processed as follows: (i) sequencing primer was removed with CUTADAPT [57], while the low-quality ends at 5' was removed using Sickle with a quality cutoff of 18. (ii) MICCA v1.7.2 [58] was then used for all analysis steps from pre-treated sequences to final Amplicon Sequence Variance (ASV) picking. The latter was performed using the UNOISE3 algorithm [59] and taxonomy was assigned using the VSEARCH [60] algorithm and the SILVA 132 database [61].

According to the presence of azurin gene in the different bacterial groups [62], the following bacterial taxa were searched and quantified in each sample from both healthy and CRC patients: *Pseudomonas* sp., (Phylum *Proteobacteria*), *Akkermansiaceae*, *Opitutaceae* (Phylum *PVC*), *Holophagales*, *Vicinamibacteria* (Phylum *Acidobacteria*), and the phyla *Bacteroidetes*, *Chloroflexi* and *Actinobacteria*.

R software version 4.2 was used to analyse these bacterial group subsets (i.e., their distribution among samples) and the whole HTS dataset, using vegan [63] and ggplot2 [64] for diversity analysis. Data of the azurin-subset community were normalized with z-score transformation prior to distance matrix calculation using the Euclidean dissimilarity index. This transformation was necessary to account for the large difference in relative abundance between the selected variables, some at the species-genus level while others at the level of entire phyla. Data of the whole HTS dataset were normalized with relative abundance transformation prior to distance matrix calculation using the Bray-Curtis dissimilarity index. In both cases, distance matrixes were used for diversity evaluation with non-metric Multidimensional Scaling (nMDS), as well their correlation was measured with Mantel test in the vegan package (9999 permutations, Pearson correlation).

Table 3. List of samples from CRC patients and healthy subjects [49] used for real-Time PCR.

Sample name	CRC patient/ healthy subject	Sample type
CM7_S	CRC patient	Saliva
CM7_F	CRC patient	Stool
CM7_B	CRC patient	Biopsy
CM8_S	CRC patient	Saliva
CM8_F	CRC patient	Stool
CM8_B	CRC patient	Biopsy
CM10_S	CRC patient	Saliva
CM10_F	CRC patient	Stool
CM10_B	CRC patient	Biopsy
CM11_S	CRC patient	Saliva
CM11_F	CRC patient	Stool
CM11_B	CRC patient	Biopsy
CM18_S	CRC patient	Saliva
CM18_F	CRC patient	Stool
CM18_B	CRC patient	Biopsy
CM19_S	CRC patient	Saliva
CM19_F	CRC patient	Stool
CM19_B	CRC patient	Biopsy
CM20_S	CRC patient	Saliva
CM20_F	CRC patient	Stool
CM20_B	CRC patient	Biopsy
CM22_S	CRC patient	Saliva
CM22_F	CRC patient	Stool
CM22_B	CRC patient	Biopsy
CM23_S	CRC patient	Saliva
CM23_F	CRC patient	Stool
CM23_B	CRC patient	Biopsy
CM24_S	CRC patient	Saliva
CM24_F	CRC patient	Stool
CM24_B	CRC patient	Biopsy
CFP1_S	healthy subject	Saliva
CFP1_F	healthy subject	Stool
CFP2_S	healthy subject	Saliva
CFP2_F	healthy subject	Stool
CFP3_S	healthy subject	Saliva
CFP3_F	healthy subject	Stool
CFP4_S	healthy subject	Saliva
CFP4_F	healthy subject	Stool
CFP6_S	healthy subject	Saliva
CFP6_F	healthy subject	Stool
CFP7_S	healthy subject	Saliva
CFP7_F	healthy subject	Stool
CFP8_S	healthy subject	Saliva
CFP8_F	healthy subject	Stool
CFP9_S	healthy subject	Saliva
CFP9_F	healthy subject	Stool
CFP10_S	healthy subject	Saliva
CFP10_F	healthy subject	Stool
CFP11_S	healthy subject	Saliva

3. Results

3.1 End-Point PCR

End-point amplifications with the six designed primer sets on the panel of bacterial strains listed in Table 2, gave different results. Fig. 1 and Table 4 summarizes the outcome of the amplifications.

An amplicon of the expected size was detected in all samples except for the primer pair "*Pseudomonas* group 1" (Fig. 1). For this reason, this primer pair was excluded from the further analyses. Each primer pair specifically amplified the azurin gene fragment of the bacterial strains belonging to its specific group, with the exception of primer pairs "*Aeromonas*", which gave amplicons not only from *Aeromonas* sp. strains 3.18, 11.45, and 11.47, but also from strains 2.13 affiliated to the genus *Pseudomonas* (Fig. 1). For this reason, also this primer pair was removed from the subsequent analysis.

The nucleotide sequence of seven randomly chosen end-point amplicon was determined and submitted to Blastx online databases for comparison with the available deposited sequences, in order to verify whether not only the fragment length, but also the amplified sequence corresponded to the azurin encoding gene. All the sequences retrieved at the lowest t-value the azurin gene, thus confirming the efficacy/specificity of the designed primer pairs and are available in the supplementary material.

3.2 Real-Time PCR

Once the azurin amplicons from each primers pair were quantified, a standard curve was constructed for each couple. Table 5 (Ref. [52–54]) shows the bacterial strains from which DNA was used for azurin amplification and standard curve construction, and also the azurin copy number calculation for the standard curves prepared for each primers pair selected for real-time PCR.

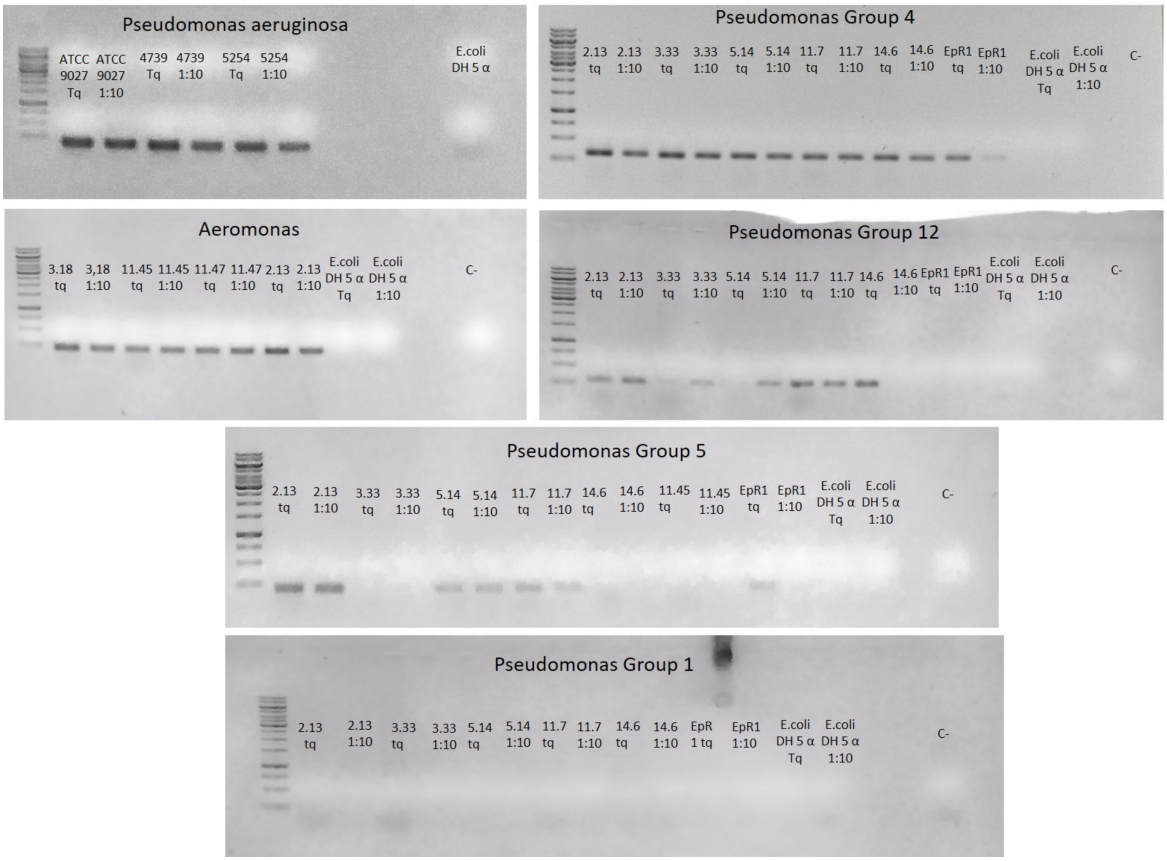

Fig. 1. End-point PCR results using the six primer pairs designed in this work. DNA were used both not diluted (Tq) and diluted (1:10). Negative controls indicated as "C-".

Table 4. Results of the azurin gene amplification through end-point PCR using the six primer pairs on a panel of bacterial strains present in the laboratory collections. YES: amplification occurred; NO: amplification not occurred; "-" reaction not tested.

	Pseudomonas aeruginosa	*Pseudomonas* group 12	*Pseudomonas* group 1	P*seudomonas* group 4	*Aeromonas*	*Pseudomonas* group 5
3.33	-	YES	NO	YES	-	NO
5.14	-	YES	NO	YES	-	YES
11.7	-	YES	NO	YES	-	YES
2.13	-	YES	NO	YES	YES	YES
14.6	-	YES	NO	YES	-	NO
3.18	-	-	-	-	YES	-
11.45	-	-	-	-	YES	-
11.47	-	-	-	-	YES	-
Ep_R1	-	NO	NO	YES	-	-
ATCC 9027	YES	-	-	-	-	-
4739	YES	-	-	-	-	-
5254	YES	-	-	-	-	-
DH5α	NO	NO	NO	NO	NO	NO

Table 5. Characteristics of the DNA used for standard curve construction in the real-time PCRs.

Primer pairs	Bacterial strain	Reference	Amplicon concentration	No. copies of amplicon in 1 µL
Pseudomonas aeruginosa	*P. aeruginosa* ATCC 9027		40 ng/µL	5.26×10^{10}
Pseudomonas group 12	2.13	[52]	1 ng/µL	3.37×10^{9}
Pseudomonas group 5	5.14	[52]	0.2 ng/µL	9×10^{8}
Pseudomonas group 4	Ep_R1	[53,54]	0.2 ng/µL	6.2×10^{8}

Table 6. Combined results of real-time PCR analysis, and detection of specific bacterial taxa in HTS results; relative abundances are expressed as % on the total reads in columns related to the seven bacterial groups analysed; numbers in the columns related to the real-time PCR primers indicate the number of azurin copies that were calculated in real-time PCR based on the standard curve construction. 1–30 rows indicate CRC patients, while 31–50 rows indicate healthy controls.

n. row			*Chloroflexi*	*Opitutaceae*	*Akkermansia*	*Pseudomonas*	*Bacteroidetes*	*Actinobacteria*	*Acidobacteria. Holophagales*	*Pseudomonas* group 4	*Pseudomonas aeruginosa*	*Pseudomonas* group 12	*Pseudomonas* group 5
1	CM7_S	Saliva	0.00	0.00	0.00	0.00	20.93	10.97	0.00				
2	CM7_F	Stool	0.00	0.00	0.02	0.00	62.00	0.08	0.00			300	9
3	CM7_B	Biopsy	0.00	0.00	0.00	0.00	16.08	5.74	0.00				9
4	CM8_S	Saliva	0.00	0.00	0.00	0.00	22.73	4.94	0.00				
5	CM8_F	Stool	0.00	0.00	0.17	0.00	68.17	0.35	0.00			300	90
6	CM8_B	Biopsy	0.00	0.00	0.42	0.05	37.84	1.17	0.00			30	
7	CM10_S	Saliva	0.01	0.00	0.00	0.00	28.77	4.62	0.00				
8	CM10_F	Stool	0.00	0.00	0.01	0.00	32.94	0.58	0.00				9
9	CM10_B	Biopsy	0.00	0.00	0.00	0.00	18.80	2.72	0.00				
10	CM11_S	Saliva	0.00	0.00	0.00	0.00	26.73	6.57	0.00				
11	CM11_F	Stool	0.00	0.00	1.42	0.00	69.22	0.28	0.00			300	90
12	CM11_B	Biopsy	0.00	0.00	0.99	0.05	24.64	9.83	0.00				
13	CM18_S	Saliva	0.00	0.00	0.00	0.00	19.51	1.67	0.00				
14	CM18_F	Stool	0.01	0.00	3.73	0.00	50.36	1.25	0.00				
15	CM18_B	Biopsy	8.22	0.00	0.02	2.63	10.17	11.03	0.00				
16	CM19_S	Saliva	0.00	0.00	0.00	0.00	16.45	18.82	0.00				
17	CM19_F	Stool	0.00	0.00	4.09	0.00	80.82	0.16	0.00			30	
18	CM19_B	Biopsy	7.43	0.08	0.15	2.15	10.39	8.51	0.15				9
19	CM20_S	Saliva	0.01	0.00	0.01	0.00	27.25	2.71	0.00				
20	CM20_F	Stool	0.01	0.00	5.80	0.00	70.98	0.79	0.00			3	
21	CM20_B	Biopsy	6.83	0.00	0.00	2.05	7.59	8.71	0.49				9
22	CM22_S	Saliva	0.00	0.00	0.00	0.00	28.20	3.41	0.00				
23	CM22_F	Stool	0.00	0.00	0.00	0.00	63.68	0.38	0.00				
24	CM22_B	Biopsy	1.61	0.05	0.00	0.16	35.47	1.76	0.04				
25	CM23_S	Saliva	0.00	0.00	0.00	0.00	22.90	7.39	0.00				
26	CM23_F	Stool	0.00	0.00	5.26	0.00	46.63	0.12	0.00			30	
27	CM23_B	Biopsy	4.50	0.00	0.03	0.79	21.52	5.29	0.10				
28	CM24_S	Saliva	0.01	0.00	0.01	0.00	11.53	11.04	0.00				
29	CM24_F	Stool	0.01	0.00	0.00	0.00	52.03	0.35	0.00			30	
30	CM24_B	Biopsy	3.57	0.00	0.00	0.62	44.20	4.54	0.00				
31	CFP1_S	Saliva	0.00	0.00	0.02	0.00	27.14	5.06	0.00				
32	CFP1_F	Stool	0.00	0.00	4.70	0.00	68.68	0.28	0.00				

Table 6. Continued.

n. row			*Chloroflexi*	*Opitutaceae*	*Akkermansia*	*Pseudomonas*	*Bacteroidetes*	*Actinobacteria*	*Acidobacteria. Holophagales*	*Pseudomonas* group 4	*Pseudomonas aeruginosa*	*Pseudomonas* group 12	*Pseudomonas* group 5
33	CFP2_S	Saliva	0.00	0.00	0.00	0.00	39.19	3.83	0.00				
34	CFP2_F	Stool	0.00	0.00	0.02	0.00	70.82	0.44	0.00			300	90
35	CFP3_S	Saliva	0.00	0.00	0.00	0.00	38.22	6.30	0.00				
36	CFP3_F	Stool	0.00	0.00	0.02	0.00	44.35	0.25	0.00			30	
37	CFP4_S	Saliva	0.00	0.00	0.00	0.00	33.96	0.99	0.00				
38	CFP4_F	Stool	0.00	0.00	0.00	0.00	25.00	0.00	0.00			300	
39	CFP6_S	Saliva	0.00	0.00	0.01	0.00	18.92	11.43	0.00				
40	CFP6_F	Stool	0.00	0.00	0.00	0.00	21.01	0.50	0.00				
41	CFP7_S	Saliva	0.01	0.00	0.01	0.00	23.51	3.26	0.00				
42	CFP7_F	Stool	0.00	0.00	4.30	0.00	20.70	1.20	0.00			30	
43	CFP8_S	Saliva	0.00	0.00	0.00	0.00	16.99	1.97	0.00				
44	CFP8_F	Stool	0.01	0.00	0.01	0.25	64.33	0.39	0.00				
45	CFP9_S	Saliva	0.00	0.00	0.00	0.00	31.37	2.80	0.00				
46	CFP9_F	Stool	0.00	0.00	0.14	0.04	69.50	0.13	0.00			300	
47	CFP10_S	Saliva	0.00	0.00	0.00	0.00	23.12	5.62	0.00				
48	CFP10_F	Stool	0.00	0.00	1.10	0.00	21.48	0.72	0.00				9
49	CFP11_S	Saliva	0.01	0.00	0.00	0.00	8.62	11.00	0.00				
50	CFP11_F	Stool	0.00	0.00	1.03	0.00	20.40	0.11	0.00				

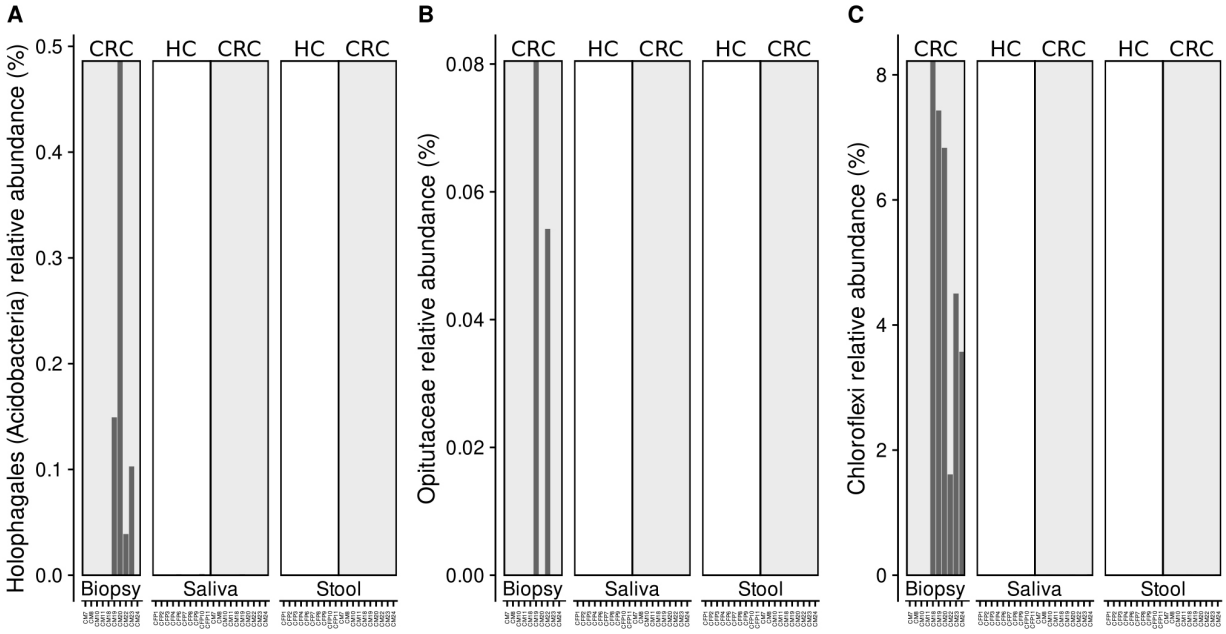

Fig. 2. Relative abundance of *Holophagales* (A), *Opitutaceae* (B) and *Chloroflexi* (C) reads detected in the samples analysed through HTS technique.

Real-time reactions revealed the presence of the azurin gene in both CRC and healthy patients as shown in Table 6. The primer pairs "*Pseudomonas* group 4" and "*Pseudomonas aeruginosa*" were not effective in detecting the azurin gene in the samples analysed. Primer pair "*Pseudomonas* group 5" gave positive results for the azurin gene in 7 CRC samples (4 samples of stool and 3 sample of biopsy) and in 2 healthy subjects (stool samples). Finally, primer pair "*Pseudomonas* group 12" successfully amplified the azurin coding gene from 8 CRC patients (7 stool samples and 1 biopsy) and 5 stool samples collected from healthy subjects (Table 6).

3.3 Distribution of the Azurin-Producing Bacterial Groups in HTS Data from CRC Patients and Healthy Controls

The relative abundances of *Pseudomonas* sp., (Phylum Proteobacteria), Akkermansiaceae, Opitutaceae (Phylum PVC), Holophagales, Vicinamibacteria (Phylum Acidobacteria), and the phyla Bacteroidetes, Chloroflexi and Actinobacteria, were evaluated in each sample through the analysis of the HTS data reported in Russo *et al.* [49]. Data obtained are resumed in Fig. 2 and Fig. 3 (Ref. [49]). It was worth of noticing that Holophagales, Opitutaceae, and Chloroflexi were detected only in samples of biopsy from CRC patients, and not in stool and saliva samples from either healthy or CRC subjects (Fig. 2).

Also, the relative abundance of *Pseudomonas* sp. (Fig. 3D) suggest that this bacterial genus is highly represented in the biopsy samples of CRC patients, while it is about completely lacking in all the other samples, except for two stool samples from healthy controls (samples CFP 8 and 9), showing a low *Pseudomonas* sp. abundance. Interestingly, while *Akkermansia* sp. is highly represented in stool samples, and slightly more abundant in CRC patients respect to healthy controls (Fig. 3A—difference not statistically significant with p-value = 0.4057), the relative abundance of *Actinobacteria* (Fig. 3B) revealed that this bacterial group is highly represented in saliva samples of both CRC and healthy subjects (no statistically significant difference of the *Actinobacteria* relative abundance between CRC and healthy subjects in Kruskal-Wallis test), as well as in CRC biopsy samples.

Finally, *Bacteroidetes* relative abundance revealed that this group is generally more represented in stool than in saliva and suggested a higher abundance in CRC patients' stool than in healthy subject, even though the difference failed to reach a statistically significance with a p value = 0.13.

Data obtained were further inspected with ordination analysis, using nMDS on the subset of bacterial groups harbouring the azurin gene (Fig. 4A) and on the whole set of HTS data (Fig. 4B). The aim of this analysis was investigating the extent to which the taxa subset harbouring azurin gene was related to the whole HTS dataset. To this aim, we firstly investigated community diversity using ordination analysis. In both cases, the ordination, provided a good representation of the real distances among samples as indicated by a stress value <0.1. A net division between the three sample types was always visible (shapes in Fig. 4), but CRC (full shapes) and healthy control (empty shapes) samples from all samples type were always in strong overlap, indicating that in both the selected subset and in the whole HTS dataset, the community mainly varied respect to different samples type. Indeed, pathology (i.e., CRC vs

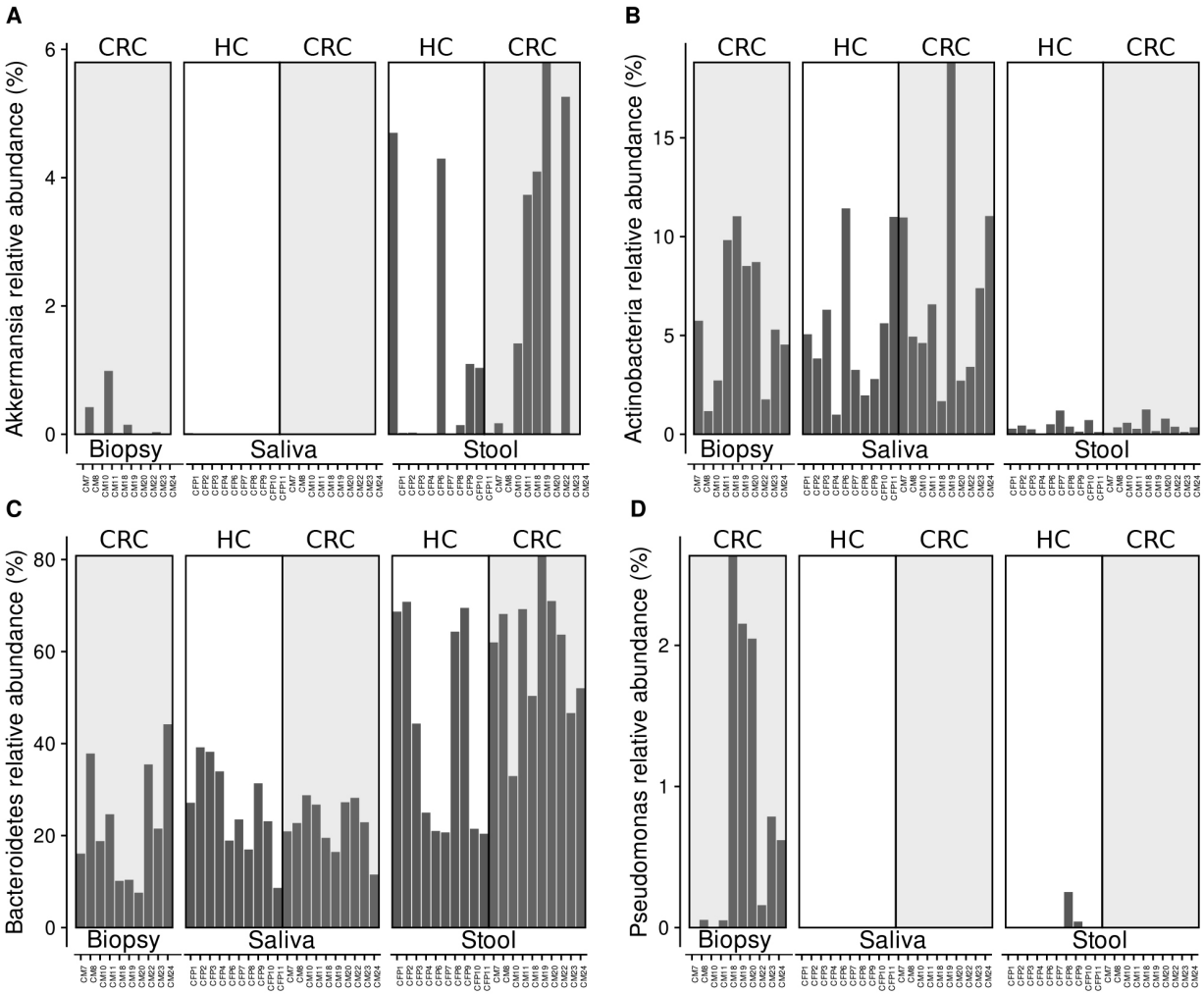

Fig. 3. Relative abundance of *Akkermansia* (A), *Actinobacteria* (B), *Bacteroidetes* (C), and *Pseudomonas* (D) reads detected in the samples analysed through HTS technique [49].

healthy) was not a significant term in PERMANOVA test on the subset of bacterial groups harbouring the azurin gene both for saliva and for stool samples (p values > 0.05).

Finally, we asked the degree of correlation of the diversity between the two datasets using Mantel test (9999 permutations, Pearson correlation measure) to obtain the overall correlation between the Euclidean distance matrix calculated on the "azurin-related" subset, and the Bray-Curtis distance matrix calculated on the whole HTS dataset. Mantel test showed a moderate but highly significant correlation between the two matrices (Mantel Pearson r = 0.3554, p-value < 0.001), indicating an unexpectedly high ability of the selected groups to recapture the whole dataset.

4. Discussion

From decades, the research of new anticancer molecules has raised great interest within the scientific community. In particular, microbial secondary metabolites are under the spotlight as promising candidates of innovative anticancer approaches. Interestingly, some of them are successfully applied as therapy for the cancer treatment as well (recently reviewed by Mohammadi *et al.* [20] resuming bacterial secondary metabolites which have been clinically used or are undergoing clinical trial). Among them, azurin synthesized from *P. aeruginosa* MTCC 2453, was demonstrated to induce tumor regression. *In vivo* experiments using Dalton's lymphoma mice model demonstrated that azurin is able to induce apoptosis [32]. Likewise, anticancer activity of azurin was demonstrated *in vitro* in gastrointestinal cancers cell lines [65]. These evidences brought to the investigation on the possible optimization of azurin formulation to improve its efficacy [13,66,67], such as the drug delivery into chitosan nanoparticles [65].

In the field of CRC, given its known environmental pathogenesis (i.e., related to unhealthy diet or lifestyle) and given the known abundance and complexity of the microbial community in its target organ, the use of bacterial and bacterial-derived (secondary) metabolites is particularly promising for innovative treatment options [68].

Stemming from those premises, in this work we have

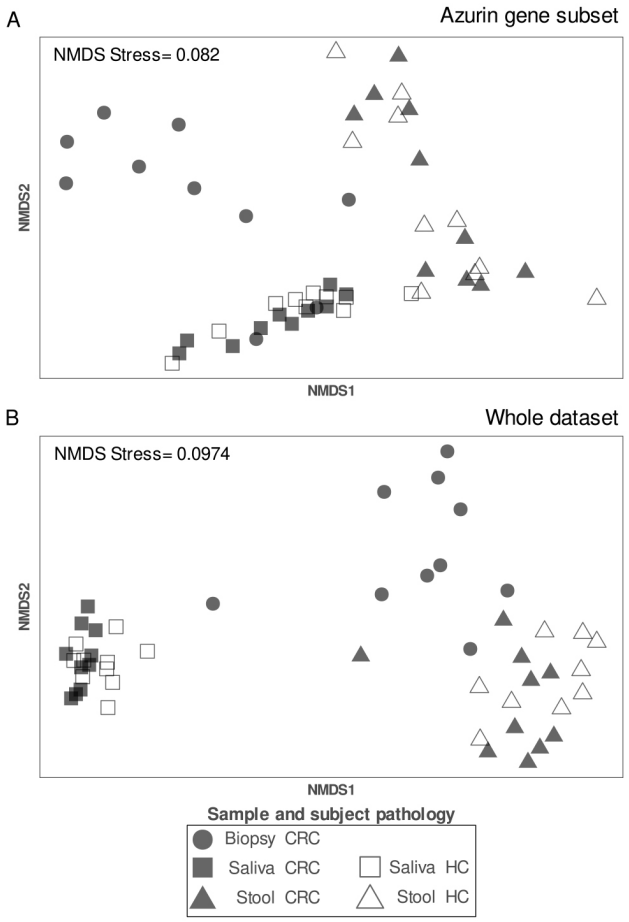

Fig. 4. Ordination plot resulting from nMDS based on Bray-Curtis dissimilarity on the (A) subset of bacterial groups harbouring the azurin gene and (B) the whole HTS dataset. Plot is annotated with stress values (i.e., a measure of the similarity of distances between samples in the reduced data of the ordination, respect to the distances between samples of the complete dataset).

evaluated the presence of azurin genes in different biological samples (i.e., saliva, stool, and biopsy) from CRC patients and healthy controls, investigating on the possible relationship existing between the disease occurrence and the different microbiota body compartments associated. Moreover, as the presence of azurin genes has been correlated to specific bacterial groups of environmental and gut origin [62], it might help in a future translation to clinical practice.

In this scenario, the construction of a valid amplification protocol for both bacterial pure cultures and biological samples is mandatory. Indeed, primer pairs are not easily available in scientific literature, and little is known about the amplification protocols of the azurin coding gene. To this purpose, our study was at first aimed at creating valid primer sets for a successful amplification and/or quantification of the gene encoding azurin in different samples. Interestingly, in a recent work [20] the amplification of azurin gene was applied to detect the differences occurring among bacterial isolates obtained from burn patients with *P. aeruginosa* infection. The authors demonstrated that the expression of azurin gene was significantly higher in the *P. aeruginosa* strains isolated from the blood of patients with systemic infections, hypothesizing an azurin role in the increased pathogenicity of the strains isolated in those patients, as well as in their ability to escape the host immune system and disseminate into the bloodstream [20].

As a further step, we analyzed HTS results obtained from previous research [49] in the light of the evidences from Gammuto *et al.* [62], this last specifically evaluating the phylogenetic distribution of azurin gene. These results allowed us to focus on a defined set of taxa known for harbouring azurin genes, rather than the entire community. This analysis revealed that bacterial taxa *Holophagales*, *Opitutaceae*, and *Chloroflexi* were only retrieved in CRC biopsy samples (Fig. 2). Although no evidence in scientific literature correlates the presence of *Holophagales* and *Opitutaceae* with tumor conditions, thus avoiding any speculation on the possible relationship of this pathology with these bacterial groups, the phylum *Chloroflexi* seems to be involved in the microbiota dysbiosis, which plays a documented key role in carcinogenesis [69].

In agreement with these observations, it has been demonstrated that the species *Chloroflexus aurantiacus* encodes for four auracyanins [70], which belong to the type 1 (T1) blue copper protein family, also known as cupredoxins; these auracyanins play a role as periplasmatic electron carriers [71]. Interestingly, it has been also highlighted that the *Chloroflexi* was one of the bacterial phyla that were significantly enriched in tissues of subsolid nodules from patients with lung adenocarcinoma [69]. A similar trend was also found in other tumor types; accordingly, microbiota alterations are associated with the different histological stages of gastric cancer [72], and higher *Chloroflexi* abundance was found in CRC biopsy samples [73]. Therefore, our observations on the *Chloroflexi* presence in CRC biopsies (Fig. 2) could direct future studies in the investigation of the possible correlations between this bacterial phylum and the azurin presence, and also in the putative relationship with cancer progression.

Another interesting result is that of the presence of *Pseudomonas* sp. bacteria only in biopsy samples, with an almost total lack in saliva and stool samples of CRC patients and healthy controls (Fig. 3). These results may be partially in agreement with the scientific literature. Indeed, despite *Pseudomonas aeruginosa* is a common colonizer of the human intestine in cancer patients facing particular clinical conditions (i.e., hospitalization, immunosuppression, antibiotic treatment, surgery, severe trauma), this bacterium increases in the number and also become more virulent and damaging to the intestinal epithelium upon surgery, injury, and severe stress [74]. Additionally, *P. aeruginosa* isolated from humans can induce intestinal pathology and cancer-related epithelial phenotypes in genetically predisposed model hosts [74]. On the other side, results from real

time PCR revealed the azurin presence from *Pseudomonas* sp. not only in biopsies but also in stool samples from both CRC and healthy patients. This incongruence might be related to the different resolution of the used molecular techniques. Indeed, HTS is aimed at a taxonomical analysis on 16S rRNA genes, while real time primers were designed on the sequence of the azurin genes from different *Pseudomonas* sp. groups. Thus, we cannot exclude *a priori* the possibility that our azurin primers might have amplified the gene from other taxonomical groups.

Recently, Yu and co-authors [75] observed a higher relative abundance of *Actinobacteria*, *Acidobacteria*, and *Chloroflexi* in the gut microbiota of myeloid leukemia compared to healthy controls; this observation confirms an alteration of the microbiota in tumor conditions. This enrichment is in line with our experimental findings, not only about *Chloroflexi*, but also regarding the presence of *Actinobacteria* in CRC biopsies (Fig. 3). Moreover, our analysis supports higher relative abundances of *Actinobacteria* in saliva samples of both healthy and CRC patients respect to stool samples. These data partially agree with results obtained analyzing other diseases; to this purpose, *Actinobacteria*, together with other phyla, were more abundant in samples from patients with periodontitis instead of in healthy controls [76].

Finally, we constructed a subset of azurin gene harbouring bacteria and tested in beta diversity analysis. The subset was intrinsically very variable in term of taxonomic level of the variables (i.e., some represented phyla, some genera) and consequently in terms of numeric count. Nevertheless, we found that this subset was able to fairly depict the entire community diversity as seen with HTS. Although this evidence is necessarily preliminary and observational due to the low number of samples involved and the strong taxonomic variability of the created subset, it still represents interesting evidence worthy of further investigation.

5. Conclusions

Overall, despite the study limitations such as the low number of recruited patients, in this work for the first time, six primer pairs targeting the bacterial azurin gene were specifically designed, tested, and validated *via* end-point and real-time PCR. Two out of the six designed primers were efficient in detecting the azurin gene in real-time PCR on human samples from CRC and healthy patients. Despite the lack of statistically significant differences between healthy and diseased patients, HTS data analysis on seven bacterial groups harbouring azurin gene in their genome highlighted a kind of "preferential" enrichment of these bacterial groups in some samples than in others (i.e., *Pseudomonas* sp., *Holophagales*, *Opitutaceae* and *Chloroflexi* in CRC biopsy, *Akkermansia* sp. in stool samples, *Actinobacteria* in saliva samples). Moreover, the subset of azurin gene-harbouring bacterial groups was representative of the entire community diversity, despite this observation needs further investigations and confirmation, on a wider number of samples.

Availability of Data and Materials

The partial 16S rRNA gene sequence data analysed in this study were previously generated and published (Russo *et al*., 2018), and are available in the GenBank Sequence Read Archive with the accession number PRJNA356414.

Author Contributions

Conceptualization—RF MI, CC; methodology—CC, MI; software—FV; validation—CC, MI; formal analysis—CC, FV, MI; investigation—RF, AA, CC, LG, MI, FV; resources—RF, AA; data curation—CC, FV, MI; writing - original draft preparation—CC, MI, FV; writing - review and editing—RF, CC, LG, MI, FV, AA, AT; supervision and project administration—RF. All authors contributed to editorial changes in the manuscript. All authors read and approved the final manuscript.

Ethics Approval and Consent to Participate

The study has received the local ethics (Toscana - area vasta centro) committee approval (CE: 11166_spe), and informed written consent has been obtained from each participant.

Acknowledgment

Not applicable.

Funding

The research was founded with a grant from the Regione Toscana, the Programma Attuativo Regionale (Toscana) funded by FAS (now FSC), that supported the project "MICpROBIMM".

Conflict of Interest

The authors declare no conflict of interest. AA is serving as one of the Editorial Board members and Guest editors of this journal. We declare that AA had no involvement in the peer review of this article and has no access to information regarding its peer review. Full responsibility for the editorial process for this article was delegated to RC.

Supplementary Material

Supplementary material associated with this article can be found, in the online version, at https://doi.org/10.31083/j.fbl2711305.

References

[1] Nauts HC, Swift WE, Coley BL. The treatment of malignant tumors by bacterial toxins as developed by the late William B. Coley, M.D., reviewed in the light of modern research. Cancer Research. 1946; 6: 205–216.

[2] Wiemann B, Starnes CO. Coley's toxins, tumor necrosis factor and cancer research: a historical perspective. Pharmacology & Therapeutics. 1994; 64: 529–564.
[3] Bernardes N, Seruca R, Chakrabarty AM, Fialho AM. Microbial-based therapy of cancer: Current progress and future prospects. Bioengineered Bugs. 2010; 1: 178–190.
[4] Karpiński TM, Adamczak A. Anticancer Activity of Bacterial Proteins and Peptides. Pharmaceutics. 2018; 10: 54.
[5] M. Fialho A, Bernardes N, M Chakrabarty A. Exploring the anticancer potential of the bacterial protein azurin. AIMS Microbiology. 2016; 2: 292–303.
[6] Marqus S, Pirogova E, Piva TJ. Evaluation of the use of therapeutic peptides for cancer treatment. Journal of Biomedical Science. 2017; 24: 21.
[7] Yaghoubi A, Khazaei M, Avan A, Hasanian SM, Cho WC, Soleimanpour S. p28 Bacterial Peptide, as an Anticancer Agent. Frontiers in Oncology. 2020; 10: 1303.
[8] Arcos-López T, Schuth N, Quintanar L. 3. The Type 1 Blue Copper Site: from Electron Transfer to Biological Function. Transition Metals and Sulfur—A Strong Relationship for Life (pp. 51–90). De Gruyter: Berlin. 2020.
[9] De Rienzo F, Gabdoulline RR, Wade RC, Sola M, Menziani MC. Computational approaches to structural and functional analysis of plastocyanin and other blue copper proteins. Cellular and Molecular Life Sciences (CMLS). 2004; 61: 1123–1142.
[10] Cruz-Gallardo I, Díaz-Moreno I, Díaz-Quintana A, Donaire A, Velázquez-Campoy A, Curd RD, *et al*. Antimalarial Activity of Cupredoxins: the interaction of Plasmodium merozoite surface protein 119 (MSP119) and rusticyanin. Journal of Biological Chemistry. 2013; 288: 20896–20907.
[11] Gao M, Zhou J, Su Z, Huang Y. Bacterial cupredoxin azurin hijacks cellular signaling networks: Protein-protein interactions and cancer therapy. Protein Science. 2017; 26: 2334–2341.
[12] Ghasemi-Dehkordi P, Doosti A, Jami M. The functions of azurin of Pseudomonas aeruginosa and human mammaglobin-a on proapoptotic and cell cycle regulatory genes expression in the MCF-7 breast cancer cell line. Saudi Journal of Biological Sciences. 2020; 27: 2308–2317.
[13] Mansour M, Ismail S, Abou-Aisha K. Bacterial delivery of the anti-tumor azurin-like protein Laz to glioblastoma cells. AMB Express. 2020; 10: 59.
[14] Nguyen C, Nguyen VD. Discovery of Azurin-Like Anticancer Bacteriocins from Human Gut Microbiome through Homology Modeling and Molecular Docking against the Tumor Suppressor p53. BioMed Research International. 2016; 2016: 1–12.
[15] Sereena MC, Sebastian D. Evaluation of Anticancer and Antihemolytic Activity of Azurin, a Novel Bacterial Protein from Pseudomonas aeruginosa SSj. International Journal of Peptide Research and Therapeutics. 2020; 26: 459–466.
[16] Choi M, Davidson VL. Cupredoxins—a study of how proteins may evolve to use metals for bioenergetic processes. Metallomics. 2011; 3: 140–151.
[17] De Rienzo F, Gabdoulline RR, Menziani MC, Wade RC. Blue copper proteins: a comparative analysis of their molecular interaction properties. Protein Science. 2000; 9: 1439–1454.
[18] Chakrabarty AM. Bacterial azurin in potential cancer therapy. Cell Cycle. 2016; 15: 1665–1666.
[19] Horio T. Terminal oxidation system in bacteria. The Journal of Biochemistry. 1958; 45: 267–279.
[20] Mohammadi Barzelighi H, Bakhshi B, Daraei B, Fazeli H, Nasr Esfahani B. Global Sequence Analysis and Expression of *Azurin* Gene in Different Clinical Specimens of Burn Patients with *Pseudomonas aeruginosa* Infection. Infection and Drug Resistance. 2020; 13: 2261–2275.
[21] Olsson MHM, Ryde U. The influence of axial ligands on the reduction potential of blue copper proteins. Journal of Biological Inorganic Chemistry. 1999; 4: 654–663.
[22] Fialho AM, Stevens FJ, Das Gupta TK, Chakrabarty AM. Beyond host–pathogen interactions: microbial defense strategy in the host environment. Current Opinion in Biotechnology. 2007; 18: 279–286.
[23] Mahfouz M, Hashimoto W, Das Gupta TK, Chakrabarty AM. Bacterial proteins and CpG-rich extrachromosomal DNA in potential cancer therapy. Plasmid. 2007; 57: 4–17.
[24] Taylor BN, Mehta RR, Yamada T, Lekmine F, Christov K, Chakrabarty AM, *et al*. Noncationic Peptides Obtained from Azurin Preferentially Enter Cancer Cells. Cancer Research. 2009; 69: 537–546.
[25] Y Yamada T, Fialho AM, Punj V, Bratescu L, Gupta TK, Chakrabarty AM. Internalization of bacterial redox protein azurin in mammalian cells: entry domain and specificity. Cellular Microbiology. 2005; 7: 1418–1431.
[26] Mehta RR, Yamada T, Taylor BN, Christov K, King ML, Majumdar D, *et al*. A cell penetrating peptide derived from azurin inhibits angiogenesis and tumor growth by inhibiting phosphorylation of VEGFR-2, FAK and Akt. Angiogenesis. 2011; 14: 355–369.
[27] Ruseska I, Zimmer A. Internalization mechanisms of cell-penetrating peptides. Beilstein Journal of Nanotechnology. 2020; 11: 101–123.
[28] Habault J, Poyet JL. Recent Advances in Cell Penetrating Peptide-Based Anticancer Therapies. Molecules. 2019; 24: 927.
[29] Sugahara KN, Teesalu T, Karmali PP, Kotamraju VR, Agemy L, Girard OM, *et al*. Tissue-Penetrating Delivery of Compounds and Nanoparticles into Tumors. Cancer Cell. 2009; 16: 510–520.
[30] Yamada T, Mehta RR, Lekmine F, Christov K, King ML, Majumdar D, *et al*. A peptide fragment of azurin induces a p53-mediated cell cycle arrest in human breast cancer cells. Molecular Cancer Therapeutics. 2009; 8: 2947–2958.
[31] Yamada T, Das Gupta TK, Beattie CW. P28-Mediated Activation of p53 in G2–M Phase of the Cell Cycle Enhances the Efficacy of DNA Damaging and Antimitotic Chemotherapy. Cancer Research. 2016; 76: 2354–2365.
[32] Ramachandran S, Mandal M. Induction of apoptosis of azurin synthesized from P. aeruginosa MTCC 2453 against Dalton's lymphoma ascites model. Biomedicine and Pharmacotherapy. 2011; 65: 461–466.
[33] Zhang Y, Zhang Y, Xia L, Zhang X, Ding X, Yan F, *et al*. Escherichia coli Nissle 1917 Targets and Restrains Mouse B16 Melanoma and 4T1 Breast Tumors through Expression of Azurin Protein. Applied and Environmental Microbiology. 2012; 78: 7603–7610.
[34] Apiyo D, Wittung-Stafshede P. Unique complex between bacterial azurin and tumor-suppressor protein p53. Biochemical and Biophysical Research Communications. 2005; 332: 965–968.
[35] Punj V, Bhattacharyya S, Saint-Dic D, Vasu C, Cunningham EA, Graves J, *et al*. Bacterial cupredoxin azurin as an inducer of apoptosis and regression in human breast cancer. Oncogene. 2004; 23: 2367–2378.
[36] Ramachandran S, Sarkar S, Mazumadar A, Mandal M. Azurin Synthesis from Pseudomonas Aeruginosa MTCC 2453, Properties, Induction of Reactive Oxygen Species, and p53 Stimulated Apoptosis in Breast Carcinoma Cells. Journal of Cancer Science and Therapy. 2011; 3: 104–111.
[37] Yamada T, Hiraoka Y, Ikehata M, Kimbara K, Avner BS, Das Gupta TK, *et al*. Apoptosis or growth arrest: Modulation of tumor suppressor p53's specificity by bacterial redox protein azurin. Proceedings of the National Academy of Sciences of the United States of America. 2004; 101: 4770–4775.
[38] Bernardes N, Ribeiro AS, Abreu S, Mota B, Matos RG, Arraiano CM, *et al*. The bacterial protein azurin impairs invasion and FAK/Src signaling in P-cadherin-overexpressing breast cancer cell models. PLoS ONE. 2013; 8: e69023.
[39] Bernardes N, Ribeiro AS, Abreu S, Vieira AF, Carreto L, Santos M, *et al*. High-throughput molecular profiling of a P-cadherin overexpressing breast cancer model reveals new targets for the anti-cancer bacterial protein azurin. The International Journal of Biochemistry and Cell Biology. 2014; 50: 1–9.
[40] Bernardes N, Garizo AR, Pinto SN, Caniço B, Perdigão C, Fer-

nandes F, *et al*. Azurin interaction with the lipid raft components ganglioside GM-1 and caveolin-1 increases membrane fluidity and sensitivity to anti-cancer drugs. Cell Cycle. 2018; 17: 1649–1666.
[41] Soleimani M, Mirmohammmad Sadeghi H, Jahanian-Najafabadi A. A Bi-Functional Targeted P28-NRC Chimeric Protein with Enhanced Cytotoxic Effects on Breast Cancer Cell Lines. Iranian Journal of Pharmaceutical Research. 2019; 18: 735–744.
[42] Yamada T, Christov K, Shilkaitis A, Bratescu L, Green A, Santini S, *et al*. P28, a first in class peptide inhibitor of cop1 binding to p53. British Journal of Cancer. 2013; 108: 2495–2504.
[43] Bernardes N, Abreu S, Carvalho FA, Fernandes F, Santos NC, Fialho AM. Modulation of membrane properties of lung cancer cells by azurin enhances the sensitivity to EGFR-targeted therapy and decreased β1 integrin-mediated adhesion. Cell Cycle. 2016; 15: 1415–1424.
[44] Lulla RR, Goldman S, Yamada T, Beattie CW, Bressler L, Pacini M, *et al*. Phase I trial of p28 (NSC745104), a non-HDM2-mediated peptide inhibitor of p53 ubiquitination in pediatric patients with recurrent or progressive central nervous system tumors: A Pediatric Brain Tumor Consortium Study. Neuro-Oncology. 2016; 18: 1319–1325.
[45] Warso MA, Richards JM, Mehta D, Christov K, Schaeffer C, Rae Bressler L, *et al*. A first-in-class, first-in-human, phase I trial of p28, a non-HDM2-mediated peptide inhibitor of p53 ubiquitination in patients with advanced solid tumours. British Journal of Cancer. 2013; 108: 1061–1070.
[46] Sánchez-Alcoholado L, Ramos-Molina B, Otero A, Laborda-Illanes A, Ordóñez R, Medina JA, *et al*. The Role of the Gut Microbiome in Colorectal Cancer Development and Therapy Response. Cancers. 2020; 12: 1406.
[47] Ternes D, Karta J, Tsenkova M, Wilmes P, Haan S, Letellier E. Microbiome in Colorectal Cancer: how to Get from Meta-omics to Mechanism? Trends in Microbiology. 2020; 28: 401–423.
[48] Tahmourespour A, Ahmadi A, Fesharaki M. The anti-tumor activity of exopolysaccharides from Pseudomonas strains against HT-29 colorectal cancer cell line. International Journal of Biological Macromolecules. 2020; 149: 1072–1076.
[49] Russo E, Bacci G, Chiellini C, Fagorzi C, Niccolai E, Taddei A, *et al*. Preliminary Comparison of Oral and Intestinal Human Microbiota in Patients with Colorectal Cancer: A Pilot Study. Frontiers in Microbiology. 2018: 8: 2699.
[50] Hall TA. BioEdit: A User-Friendly Biological Sequence Alignment Editor and Analysis Program for Windows 95/98/NT. Nucleic Acids Symposium Series. 1999; 41: 95–98.
[51] Weissensteiner T, Griffin HG, G. A. PCR Technology: Current Innovations, 2nd edn. CRC Press. 2004.
[52] Chiellini C, Miceli E, Bacci G, Fagorzi C, Coppini E, Fibbi D, *et al*. Spatial structuring of bacterial communities in epilithic biofilms in the Acquarossa river (Italy). FEMS Microbiology Ecology. 2018; 94.
[53] Chiellini C, Maida I, Emiliani G, Mengoni A, Mocali S, Fabiani A, *et al*. Endophytic and rhizospheric bacterial communities isolated from the medicinal plants Echinacea purpurea and Echinacea angustifolia. International Microbiology . 2014; 17: 165–174.
[54] Maggini V, Presta L, Miceli E, Fondi M, Bosi E, Chiellini C, *et al*. Draft Genome Sequence of *Pseudomonas* sp. Strain Ep R1 Isolated from *Echinacea purpurea* Roots and Effective in the Growth Inhibition of Human Opportunistic Pathogens Belonging to the *Burkholderia cepacia* Complex. Genome Announcements. 2017; 5: e00351–17.
[55] Checcucci A, Azzarello E, Bazzicalupo M, Galardini M, Lagomarsino A, Mancuso S, *et al*. Mixed Nodule Infection in Sinorhizobium meliloti-Medicago sativa Symbiosis Suggest the Presence of Cheating Behavior. Frontiers in Plant Science. 2016; 7: 835.
[56] Vitali F, Colucci R, Di Paola M, Pindo M, De Filippo C, Moretti S, *et al*. Early melanoma invasivity correlates with gut fungal and bacterial profiles. British Journal of Dermatology. 2022; 186: 106–116.
[57] Martin M. Cutadapt removes adapter sequences from high-throughput sequencing reads. EMBnet. Journal. 2011; 17: 10–12.
[58] Albanese D, Fontana P, De Filippo C, Cavalieri D, Donati C. MICCA: a complete and accurate software for taxonomic profiling of metagenomic data. Scientific Reports. 2015; 5: 9743.
[59] Edgar RC. UNOISE2: improved error-correction for Illumina 16S and ITS amplicon sequencing. bioRxiv. 2016. (Preprint)
[60] Rognes T, Flouri T, Nichols B, Quince C, Mahé F. VSEARCH: a versatile open source tool for metagenomics. PeerJ. 2016; 4: e2584.
[61] Quast C, Pruesse E, Yilmaz P, Gerken J, Schweer T, Yarza P, *et al*. The SILVA ribosomal RNA gene database project: improved data processing and web-based tools. Nucleic Acids Research. 2013; 41: D590–D596.
[62] Gammuto L, Chiellini C, Iozzo M, Fani R, Petroni G. The Azurin Coding Gene: Origin and Phylogenetic Distribution. Microorganisms. 2021; 10: 9.
[63] Oksanen J, Simpson G, Blanchet FG, Kindt R, Legendre P, Minchin P, *et al*. Vegan Community Ecology Package. R Package Version 2.6-2. 2022. Available at: https://compmetagen.github.io/micca/ (Accessed: 1 November 2022).
[64] Wickham H. ggplot2: Elegant Graphics for Data Analysis. Springer-Verlag: New York. 2016.
[65] Al-Hazmi NE, Naguib DM. Microbial Azurin Immobilized on Nano-Chitosan as Anticancer and Antibacterial Agent against Gastrointestinal Cancers and Related Bacteria. Journal of Gastrointestinal Cancer. 2022; 53: 537–542.
[66] Alqahtani MA, Al Othman MR, Mohammed AE. Bio fabrication of silver nanoparticles with antibacterial and cytotoxic abilities using lichens. Scientific Reports. 2020; 10: 16781.
[67] Borrelli A, Tornesello AL, Tornesello ML, Buonaguro FM. Cell Penetrating Peptides as Molecular Carriers for Anti-Cancer Agents. Molecules. 2018; 23: 295.
[68] Ebrahimzadeh S, Ahangari H, Soleimanian A, Hosseini K, Ebrahimi V, Ghasemnejad T, *et al*. Colorectal cancer treatment using bacteria: focus on molecular mechanisms. BMC Microbiology. 2021; 21: 218.
[69] Ma Y, Qiu M, Wang S, Meng S, Yang F, Jiang G. Distinct tumor bacterial microbiome in lung adenocarcinomas manifested as radiological subsolid nodules. Translational Oncology. 2021; 14: 101050.
[70] King JD, McIntosh CL, Halsey CM, Lada BM, Niedzwiedzki DM, Cooley JW, *et al*. Metalloproteins Diversified: the Auracyanins are a Family of Cupredoxins that Stretch the Spectral and Redox Limits of Blue Copper Proteins. Biochemistry. 2013; 52: 8267–8275.
[71] McManus JD, Brune DC, Han J, Sanders-Loehr J, Meyer TE, Cusanovich MA, *et al*. Isolation, characterization, and amino acid sequences of auracyanins, blue copper proteins from the green photosynthetic bacterium Chloroflexus aurantiacus. Journal of Biological Chemistry. 1992; 267: 6531–6540.
[72] Wang Z, Gao X, Zeng R, Wu Q, Sun H, Wu W, *et al*. Changes of the Gastric Mucosal Microbiome Associated With Histological Stages of Gastric Carcinogenesis. Frontiers in Microbiology. 2020; 11: 997.
[73] Lu Y, Chen J, Zheng J, Hu G, Wang J, Huang C, *et al*. Mucosal adherent bacterial dysbiosis in patients with colorectal adenomas. Scientific Reports. 2016; 6: 26337.
[74] Markou P, Apidianakis Y. Pathogenesis of intestinal Pseudomonas aeruginosa infection in patients with cancer. Frontiers in Cellular and Infection Microbiology. 2014; 3: 115.
[75] Yu D, Yu X, Ye A, Xu C, Li X, Geng W, *et al*. Profiling of gut microbial dysbiosis in adults with myeloid leukemia. FEBS Open Bio. 2021; 11: 2050–2059.
[76] Lundmark A, Hu YOO, Huss M, Johannsen G, Andersson AF, Yucel-Lindberg T. Identification of Salivary Microbiota and Its Association With Host Inflammatory Mediators in Periodontitis. Frontiers in Cellular and Infection Microbiology. 2019; 9: 216.